5934 *Biochemistry* **2009,** *48,* 5934–5942
DOI: 10.1021/bi900521n

BIOCHEMISTRY
including biophysical chemistry & molecular biology
Article

Model of the Exofacial Substrate-Binding Site and Helical Folding of the Human Glut1 Glucose Transporter Based on Scanning Mutagenesis[†]

Mike Mueckler* and Carol Makepeace

Department of Cell Biology, Washington University School of Medicine, 660 South Euclid Avenue, St. Louis, Missouri 63110

Received March 26, 2009; Revised Manuscript Received April 29, 2009

ABSTRACT: Transmembrane helix 9 of the Glut1 glucose transporter was analyzed by cysteine-scanning mutagenesis and the substituted cysteine accessibility method (SCAM). A cysteine-less (C-less) template transporter containing amino acid substitutions for the six native cysteine residues present in human Glut1 was used to generate a series of 21 mutant transporters by substituting each successive residue in predicted transmembrane segment 9 with a cysteine residue. The mutant proteins were expressed in *Xenopus* oocytes, and their specific transport activities were directly compared to that of the parental C-less molecule whose function has been shown to be indistinguishable from that of native Glut1. Only a single mutant (G340C) had activity that was reduced (by 75%) relative to that of the C-less parent. These data suggest that none of the amino acid side chains in helix 9 is absolutely required for transport function and that this helix is not likely to be directly involved in substrate binding or translocation. Transport activity of the cysteine mutants was also tested after incubation of oocytes in the presence of the impermeant sulfhydryl-specific reagent, *p*-chloromercuribenzene sulfonate (pCMBS). Only a single mutant (T352C) exhibited transport inhibition in the presence of pCMBS, and the extent of inhibition was minimal (11%), indicating that only a very small portion of helix 9 is accessible to the external solvent. These results are consistent with the conclusion that helix 9 plays an outer stabilizing role for the inner helical bundle predicted to form the exofacial substrate-binding site. All 12 of the predicted transmembrane segments of Glut1 encompassing 252 amino acid residues and more than 50% of the complete polypeptide sequence have now been analyzed by scanning mutagenesis and SCAM. An updated model is presented for the outward-facing substrate-binding site and relative orientation of the 12 transmembrane helices of Glut1.

The members of the GLUT/SLC2A family are membrane proteins that mediate the facilitative transfer of sugars across cellular membranes (*1*). These proteins belong to the major facilitator superfamily (MFS)[1] that contains nearly 3600 members in all three Kingdoms and represents the largest superfamily of membrane transporters (*2*−*4*). GLUT proteins and other MFS proteins are ubiquitously expressed and have been discovered in virtually every organism examined. At least five of the 14 mammalian GLUT proteins are glucose transporters that are expressed and regulated in a cell-specific fashion and that play distinct roles in cellular and organismal glucose homeostasis (*5*, *6*). Because glucose is an important or essential nutrient for most mammalian cells, defects in its transport are associated with several disease states, including diabetes (*7*), Glut1 deficiency syndrome (*8*), and Fanconi-Bickel disease (*9*). Most of the available kinetic and biophysical data suggest that GLUT proteins operate via an alternating conformation mechanism (*10*, *11*), although their kinetic behavior can be altered by various factors (*12*−*15*). Despite the physiological importance of these proteins, virtually nothing is known at the molecular level about the mechanism by which they bind and transport their substrates across lipid bilayers.

Glut1 was the first mammalian glucose transporter to be purified (*16*) and cloned (*17*, *18*) and is one of the most intensively investigated of all membrane transporters. It is widely expressed in mammalian cells, often in conjunction with other glucose transporter isoforms, and is the major glucose carrier of human erythrocytes and brain endothelium (*19*, *20*). It also appears to play an important role in the uptake of reduced dehydroascorbate in certain cells (*21*). Glut1 is a protein of 492 amino acid residues and contains a single N-linked oligosaccharide (*17*). Analysis of the amino acid sequence predicted the presence of 12 membrane-spanning domains, and this has been confirmed by glycosylation scanning mutagenesis studies (*22*) and is consistent with the results of proteolytic digestion experiments (*23*). These observations indicate that ~50% of the molecule is embedded in the lipid bilayer. Evidence suggests that Glut1 may function as an oligomer in some cell types, including human erythrocytes (*24*, *25*).

[†]This research was supported by a grant from the National Institutes of Health (R01 DK43695) and by the Diabetes Research and Training Center at Washington University.

*To whom correspondence should be addressed. Telephone: (314) 362-4160. Fax: (314) 362-7463. E-mail: mmueckler@wustl.edu.

[1]Abbreviations: MFS, major facilitator superfamily; pCMBS, *p*-chloromercuribenzene sulfonate; NEM, *N*-ethylmaleimide; SCAM, substituted cysteine accessibility method; C-less Glut1, cysteine-less Glut1; single-C mutant, single-cysteine mutant.

Published on Web 05/18/2009

Scanning mutagenesis studies have been reported for 11 of the 12 predicted transmembrane helices of Glut1 (*26*−*36*). These studies, together with other site-specific mutagenesis experiments (*37*−*46*), have identified several amino acid residues that appear to be critical for substrate binding or translocation. Along with homology modeling (*47*) based on the known structures of two bacterial transporters, the lac permease (*48*) and glycerol-3-P antiporter (*49*), scanning mutagenesis combined with the substituted cysteine accessibility method (SCAM) has helped in the formulation of models for the bundling and orientation of the 12 predicted transmembrane segments and the substrate-binding site in the exofacial configuration of the transporter.

Herein, we report the results of cysteine-scanning mutagenesis and SCAM analysis of transmembrane segment 9 of Glut1, the last membrane domain of the transporter to be analyzed by these procedures. The results are consistent with a model in which helix 9 is one of four outer helices that stabilize an inner bundle of eight helices that form the substrate-binding site. The cumulative experimental data are discussed with reference to a published structural model based on homology to bacterial transporters.

EXPERIMENTAL PROCEDURES

Materials. Imported female African *Xenopus laevis* frogs were purchased from *Xenopus* Express (Homosassa, FL), [^{3}H]-2-Deoxyglucose and diguanosine triphosphate were purchased from Amersham Pharmacia Biotech (Arlington Heights, IL). Megascript RNA synthesis kits were purchased from Ambion Inc. (Austin, TX), and Transformer Site-Directed mutagenesis kits were obtained from Clontech (Palo Alto, CA).

General Procedures. Procedures for the site-directed mutagenesis and sequencing of human Glut1 cDNA and the in vitro transcription and purification of Glut1 mRNAs (*50*), isolation, microinjection, and incubation of *Xenopus* oocytes (*51*), preparation of purified oocyte plasma membranes and indirect immunofluorescence laser confocal microscopy (*39*), SDS−polyacrylamide gel electrophoresis and immunoblotting with the Glut1 C-terminal antibody (*38*), and 2-deoxyglucose uptake measurements (*52*), have been described in detail previously.

Treatment with pCMBS. Stage 5 *Xenopus* oocytes were injected with 50 ng of wild-type or mutant Glut1 mRNA. Two days after injection, groups of ~20 oocytes were incubated for 15 min in the presence or absence of the indicated concentrations of *p*-chloromercuribenzene sulfonate (pCMBS), in Barth's saline at 22 °C. The 100× concentrated reagent stock was prepared in 100% dimethyl sulfoxide, and control oocytes were treated with the appropriate concentration of vehicle alone. After a 15 min incubation period, the oocytes were washed four times in Barth's saline and then used for the determination of [^{3}H]-2-deoxyglucose uptake (50 μM, 30 min at 22 °C).

Specific Activity Determinations. Membranes were prepared 2 days following injection of 50 ng of mutant RNA per oocyte. Western blot analysis of each of the mutant transporters was performed on ~1 μg of total membrane protein, and the intensity of the upper Glut1 band, representing the fully glycosylated form of the protein present in the plasma membrane, was quantified by scanning densitometry using a Molecular Dynamics Phosphorimager SI. Absolute expression levels were determined on the basis of a standard curve derived using previously titered aliquots of human erythrocyte membrane analyzed on the same blots. Analysis was performed using ImageQuant NT (version 4.0). The [^{3}H]-2-DOG uptake (picomoles per oocyte per 30 min) of each mutant was concomitantly determined in each set of experiments. Specific activity is expressed as the 2-deoxyglucose uptake per nanogram of mutant Glut1 protein expressed per microgram of total oocyte membrane protein, and the data were then normalized by assigning the uptake activity of the parental C-less protein a value of 1.0. In one instance (G343C), because of the low expression level of the mutant, expression levels of C-less Glut1 and the mutant were titered by injecting variable amounts of their corresponding mRNAs. The relative specific activity was then determined on the basis of the calculations obtained at similar levels of protein expression.

Statistical Analysis. Uptake data were analyzed for statistical significance using the two-tailed, unpaired Student's *t* test.

RESULTS AND DISCUSSION

Eleven of the 12 predicted transmembrane segments in the human Glut1 glucose transporter have previously been analyzed by cysteine-scanning mutagenesis and the substituted cysteine accessibility method (*26*−*36*). The former analysis permits identification of amino acid residues that are critical for transport activity, and the latter analysis identifies residues that are accessible to the external solvent, enabling a determination of the relative orientation of the transmembrane helices. The cDNA region of Glut1 encoding helix 9, the final Glut1 transmembrane segment to be analyzed by these procedures, was subjected to site-directed mutagenesis to create a series of 21 mutants with single cysteine substitutions (single-C mutants) along the helix. The mutations were generated using a parental Glut1 cDNA template in which all six native cysteine codons were altered to encode either glycine or serine residues (*30*, *53*). The resulting cysteine-less (C-less) Glut1 protein is fully functional when expressed in *Xenopus* oocytes. Helix 9 is presented in helical wheel format in Figure 1. It is the second most hydrophobic helix in Glut1. The specific mutations introduced into C-less Glut1 to produce the 21 helix 9 single-C mutants are listed in Table 1.

Synthetic mRNAs encoding each of the single-C mutants and the parental C-less Glut1 molecule were injected into *X. laevis* oocytes, and the expression and function of the mutant transporters were assessed 48 h later. Figure 2A shows representative confocal immunofluorescent micrographs of sections of oocytes expressing each of the mutants and stained with an antibody that recognizes the cytoplasmic C-terminus of Glut1. All of the mutants were detected in the oocyte plasma membrane and in internal membrane structures. As we have reported previously (*50*), Glut1 expressed in oocytes appeared as two broad bands by immunoblot analysis (Figure 2B). The lower band represents core glycosylated protein that had not yet traversed the Golgi apparatus. The upper band represents fully glycosylated transporter protein that had largely matured to the plasma membrane. The relative prominence of the lower bands is due to the extremely slow transit time of Glut1 through the early biosynthetic compartments of oocytes (*50*). As observed in many previous experiments (*26*−*36*), the expression levels of the different mutants were somewhat variable. The upper bands were quantified by comparison to the previously determined Glut1 content of red blood cell membranes loaded as standards on the same gels. The absolute amount of Glut1 detected in the oocyte plasma membranes was used to normalize the mutant transporter activity levels (see below).

The function of the mutant transporters was assessed by measuring the uptake of [^{3}H]-2-deoxyglucose. Figure 3 shows

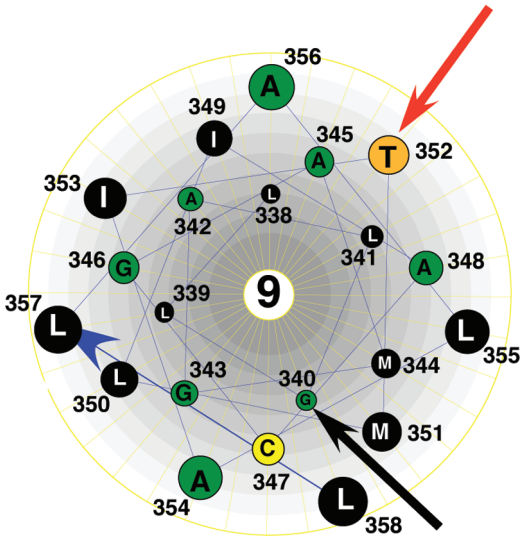

FIGURE 1: Helical wheel representation of helix 9. Transmembrane helix 9 of Glut1 viewed from the exoplasmic surface of the membrane. Amino acids are represented by the single-letter code. The red arrow points to the residue where cysteine substitution resulted in an inhibition of transport activity, and the black arrow points to the single residue that is exposed to the external solvent according to pCMBS reactivity.

uptake data after normalization to account for different levels of expression of the single-C mutants. The uptake values are compared in each case to that of the C-less parental protein analyzed using the same batches of oocytes. Only a single mutant, G340C, exhibited a statistically significant reduced specific activity relative to the C-less control. G343C protein was expressed at very low levels relative to C-less Glut1 in oocytes. Therefore, to accurately determine the activity of this mutant relative to the control, we injected different levels of C-less Glut1 and G343C mRNAs into oocytes to obtain varying levels of expression of the two proteins. The specific transport activities of G343C and the C-less control were then compared directly in independent experiments at very similar levels of protein expression. These are the results shown in Figure 3 for G343C.

The accessibility of the helix 9 residues to the external solvent was assessed by measuring [^{3}H]-2-deoxyglucose in oocytes after incubation in the presence or absence of the sulfhydryl-specific reagent, *p*-chloromercuribenzene sulfonate (pCMBS) (Figure 4). Reaction of pCMBS adds a bulky charged aromatic group to accessible cysteine side chains and inhibits transport activity to varying degrees, depending on the residue (*37*). The activity of only one mutant, T352C, was inhibited after incubation of oocytes in pCMBS, and the magnitude of the inhibition was very modest (~10%). V165C, a helix 5 mutant, is a well-characterized positive control for the pCMBS reaction (*37*). Transmembrane helices that appear to comprise the inner helical bundle and are thus predicted to have faces that are in direct contact with the external solvent contain between four and eight pCMBS reactive residues (*26*−*36*). These results are consistent with helix 9 acting as an outer stabilizing helix that has minimal contact with the exoplasmic fluid.

With the analysis of helix 9 described in this study, all 252 amino acid residues comprising the 12 predicted transmembrane segments of human Glut1 have been subjected to cysteine-scanning mutagenesis and SCAM analysis. These data are summarized schematically in Figures 5 and 6. Forty-five of the 252 predicted transmembrane residues were accessible to pCMBS

Table 1: Mutations Used To Create Helix 9 Single-Cysteine Mutants[a]

residue	amino acid change	codon change
338	Leu → Cys	CTC → TGC
339	Ile → Cys	ATA → TGC
340	Gly → Cys	GGC → TGC
341	Leu → Cys	CTC → TGC
342	Ala → Cys	GTC → TGC
343	Gly → Cys	GGC → TGC
344	Met → Cys	ATG → TGC
345	Ala → Cys	GCG → TGC
346	Gly → Cys	GGT → TGC
347	Ser → Cys	AGT → TGC
348	Ala → Cys	GCC → TGC
349	Ile → Cys	ATA → TGC
350	Leu → Cys	CTC → TGC
351	Met → Cys	ATG → TGC
352	Thr → Cys	ACC → TGC
353	Ile → Cys	ATC → TGC
354	Ala → Cys	GCG → TGC
355	Leu → Cys	CTA → TGC
356	Ala → Cys	GCA → TGC
357	Ile → Cys	CTG → TGC
358	Ile → Cys	CTG → TGC

[a] cDNA encoding cysteine-less (C-less) human Glut1 was subjected to site-directed mutagenesis, creating a series of 21 mutant cDNAs in which each of the 21 residues within transmembrane helix 9 was individually changed to cysteine. Residue refers to the amino acid numbering for human Glut1 given in ref (*17*). Amino acids are designated by the three-letter code.

from the external solvent (purple residues in Figure 5 and numbered residues in Figure 6). The results permit a crude but reliable approximation of the relative orientation of most of the transmembrane helices in the exofacial conformation of the transporter. The data are mostly consistent with a basic model for the helical packing of Glut1 (*32*, *47*) that is similar to the known crystal structures of the *Escherichia coli* lac permease (*48*), glycerol-3-P antiporter (*49*), and EmrD multidrug transporter (*54*) (see Figures 5 and 6) in which a central aqueous cavity formed by eight inner helices is stabilized by four outer helices. Helix 4 exhibited no pCMBS-sensitive residues, but the orientation shown in Figure 6 is consistent with the results of chemical cross-linking experiments involving dicysteine mutants (ref (*55*); see the discussion below). The orientation of helices 1 and 12 could not be assigned unambiguously because their pCMBS sensitivity exhibited no periodicity and their reactive residues probably lie outside of the membrane within the exoplasmic fluid (see the discussion below). They were oriented in the most thermodynamically favorable way such that their polar side chains face either the aqueous cavity or an adjacent helix and that only hydrophobic side chains directly face the fatty acyl core of the bilayer.

It is important to emphasize that the crystal structures appear to represent the cytoplasmic-facing orientations of the two bacterial transporters and that the SCAM results summarized in Figures 5 and 6 apply to the exoplasmic-facing orientation of Glut1. The latter assertion follows from the fact that pCMBS is membrane impermeant (*56*) along with the strong preference for reactivity with Glut1 residues that are predicted to reside in the exofacial halves of the 12 transmembrane segments. The crystal structures of the three bacterial transporters indicate that their prominent cytoplasmic substrate-binding cavities are tightly sealed off at the periplasmic face of the membrane, strongly suggesting a carrier model for transport function in which a substrate-binding site (or two distinct sites) are alternately

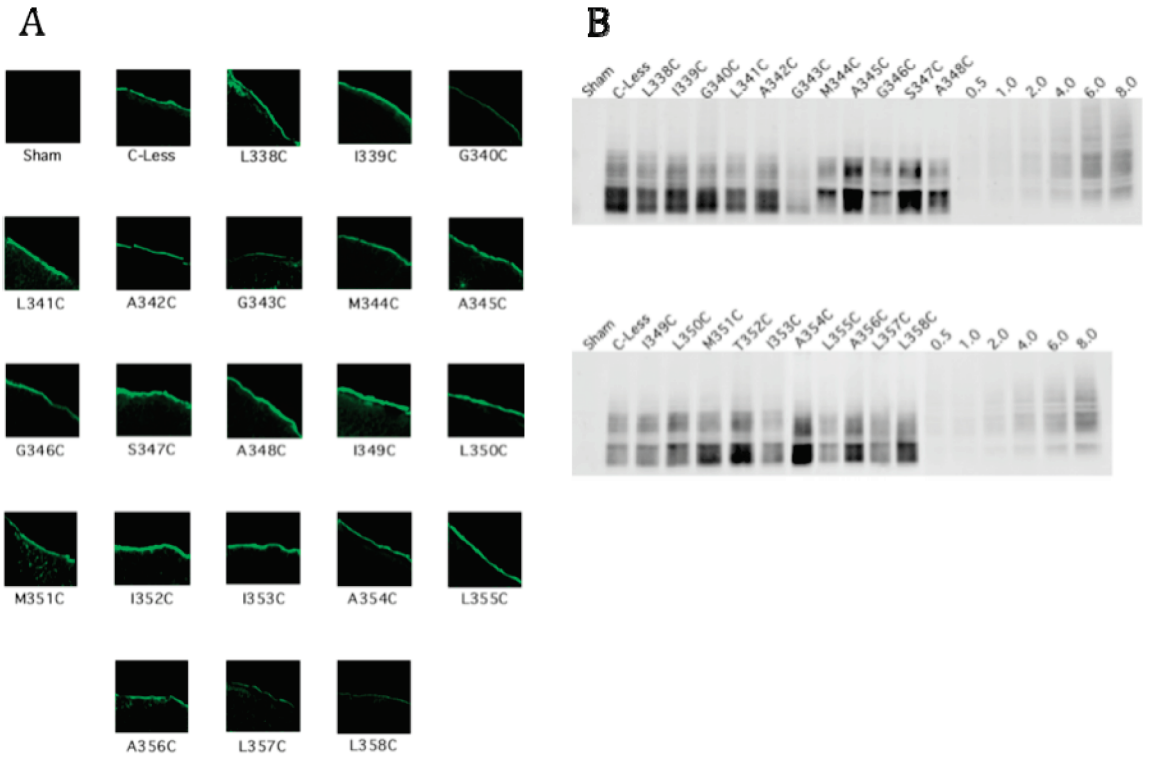

FIGURE 2: Expression of helix 9 single-C mutant transporters in *Xenopus* oocytes. Stage 5 *Xenopus* oocytes were injected with 50 ng of wild-type, C-less, or mutant C-less mRNAs; 2 days later, frozen sections were prepared and analyzed by indirect immunofluorescence laser confocal microscopy, or oocytes were used to prepare purified membrane fractions for immunoblot analysis. (A) Confocal micrographs of oocytes expressing each of the 21 single-C mutants. (B) Immunoblots of 10 μg of total oocyte membrane protein loaded per lane. Rabbit antiserum A674 raised against the 15 C-terminal residues of human Glut1 was used at a 1:500 dilution. Numbers above the lanes at the right represent the amounts in nanograms of human erythrocyte Glut1 loaded in each lane as a quantitative standard.

exposed at opposite faces of the membrane in two mutually exclusive transporter conformations (*57*). An alternating conformation/access model is also strongly suggested by the presence of a bound high-affinity disaccharide substrate within the cytoplasmic cavity of crystallized lac permease and the absence of bound ligand at the periplasmic face of the membrane (*48*, *57*). An alternating access model for glucose transport is supported by a large body of kinetic and biophysical data collected over the course of several decades (discussed in refs (*10*), (*58*), and (*59*)). Although kinetic anomalies have been observed for Glut1 (*12*), it is unclear to what extent these reflect the basic transport mechanism as opposed to regulatory phenomena or experimental limitations. It is also noteworthy that Glut4 exhibits simple symmetric carrier kinetics in rat adipocytes (*60*), consistent with an alternating access carrier model. It seems unlikely that two closely related mammalian glucose transporters would exhibit fundamentally different mechanisms.

Three of the four predicted outer helices of Glut1 (helices 3, 6, and 9) possess only a single pCMBS-sensitive residue, consistent with very limited accessibility to the external solvent. The exception is helix 12, which contains five pCMBS-sensitive residues. The five reactive residues in helix 12 are contiguous and are predicted to lie very near the exoplasmic end of the helix (see Figures 5 and 6). It is therefore probable that these residues reside outside the lipid bilayer in direct contact with the external fluid when the transporter is in its exoplasmic configuration. Seven of the eight predicted inner helices possess between four and eight residues that are reactive with pCMBS, most of which lie in the exoplasmic halves of their respective helices. These data are consistent with solvent-accessible helical faces that line a putative exoplasmic substrate-binding cavity analogous to the cytoplasmic substrate binding cavities evident in the crystal structures of the bacterial transporters. The sole exception is helix 4, which does not possess any pCMBS-sensitive residues. This observation strongly suggests that helix 4 has little if any exposure to the external solvent. The four pCMBS-reactive residues in helix 1 are contiguous and, like the pCMBS-sensitive residues in helix 12, are predicted to lie at the extreme exoplasmic end of the helix (see Figures 5 and 6). It is therefore probable that these residues are positioned in the extracellular fluid outside of the membrane when the transporter is in its exofacial configuration and that the bulk of helix 1 may be shielded from the exoplasmic fluid in the external orientation.

Helix 4 lines the aqueous cavity present in the cytoplasmic configurations of the lac permease (*48*) and glycerol-3-P antiporter (*49*) and participates directly in substrate binding in the case of the lac permease. If we assume that the basic cytoplasmic folding pattern of the two bacterial transporters is conserved in Glut1 (*32*, *47*), then the lack of solvent accessibility of helix 4 in the exofacial configuration suggests that the exoplasmic helical bundling patterns of the MFS transporters may differ from that of their cytoplasmic structures. Additional evidence in support of this possibility is provided by chemical cross-linking experiments conducted on dicysteine mutant Glut1 molecules expressed in oocytes (*55*). This study demonstrated that Leu325 and Val328 near the cytoplasmic end of helix 8 are positioned within ~6 Å of Gly145 and Ser148, both of which are located near the cytoplasmic end of helix 4. These two pairs of residues are predicted to be positioned much further apart (~26 Å) in the Glut1 structure modeled on the cytoplasmic configuration of the glycerol-3-P antiporter (*49*). Thus, either this Glut1 model is not accurate, or the cytoplasmic and exoplasmic structures of the transporter

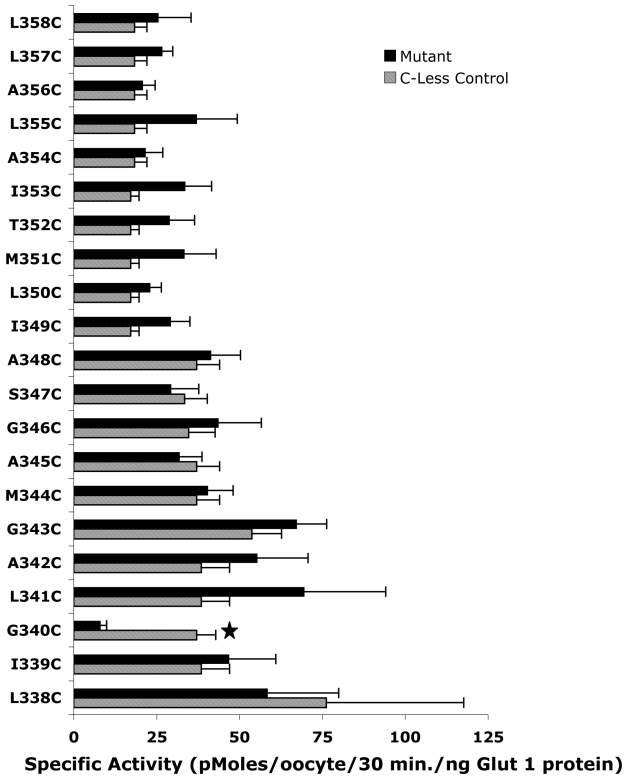

FIGURE 3: 2-Deoxyglucose uptake activity of helix 9 single-C mutants. [^{3}H]-2-Deoxyglucose uptake (50 μM, 30 min at 22 °C) and the plasma membrane content of each single-C mutant were quantitated 2 days after injection of mRNAs. Results represent the mean ± standard error of 5−10 independent experiments, each experiment employing 15−20 oocytes per experimental group. The star denotes a p of <0.001 for the single-C mutant compared to parental C-less Glut1. Background values observed in sham-injected oocytes were subtracted.

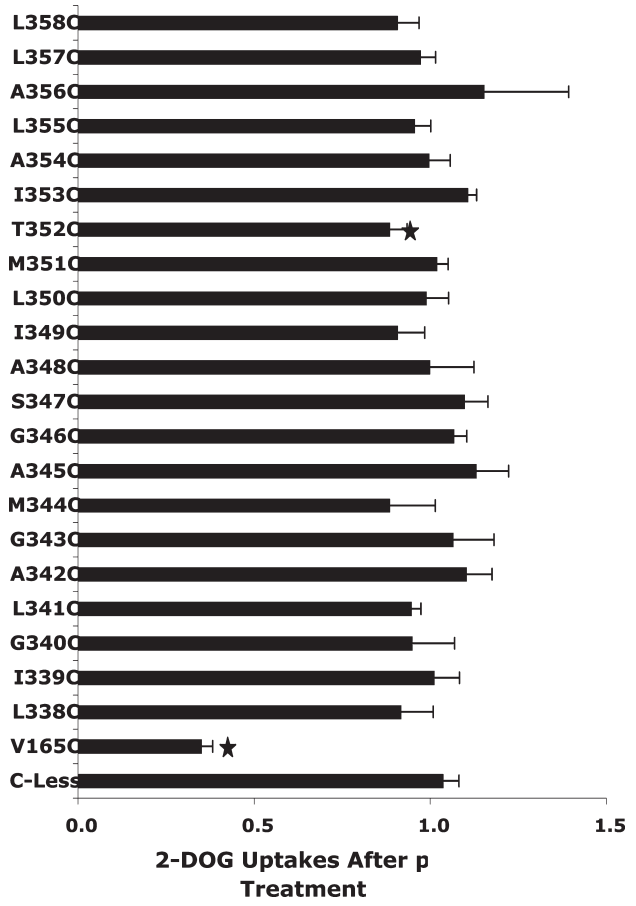

FIGURE 4: Effect of pCMBS on the transport activity of helix 9 single-C mutants. Three days after injection of mRNAs, groups of 15−20 oocytes were incubated in the presence or absence of 0.5 mM pCMBS in Barth's saline at 22 °C for 15 min. Oocytes were washed four times in Barth's saline and then subjected to 2-deoxyglucose uptake measurements under the conditions described in the legend of Figure 3. Results represent the mean ± standard error of 5−11 independent experiments, each experiment employing 15−20 oocytes per experimental group. Data are expressed as relative uptake activity, i.e., uptake observed in the presence of pCMBS divided by the uptake observed in the absence of pCMBS. C-less represents the parental cysteine-less Glut1 construct. V165C is a well-characterized positive control whose activity is inhibited by pCMBS (*37*). A star denotes a p of <0.05, activity with vs without prior incubation in the presence of pCMBS.

differ considerably. If the modeling is accurate with respect to the positioning of these two pairs of residues, then the cross-linking data presumably reflect the exoplasmic configuration of Glut1 in which an exofacially exposed cavity is sealed off at the cytoplasmic end, thus explaining the close apposition of the cytoplasmic ends of helices 4 and 8. A similar conclusion was reached in a comparison of chemical cross-linking data obtained on dicysteine mutants of the lac permease and the cytoplasmic-oriented crystal structures (*61*); i.e., the cross-linking data indicate the existence of a conformation of the permease that is distinct from the crystal structure.

What experimental evidence exists regarding the exofacial substrate-binding site of Glut1? Elegant studies using a series of deoxy, epimeric, halogeno, and *O*-alkyl glucose analogues suggest that the transporter forms hydrogen bonds with glucose at the C-1, C-3, C-4, and possibly the C-6 and ring oxygen positions (*62*, *63*). Additionally, glucose binding appears to be stabilized by a hydrophobic interaction between C-6 and an aromatic side chain of the transporter (*62*). It is not known whether all of the interactions between the sugar and Glut1 occur simultaneously in the exofacial cavity. It is possible that some interactions occur sequentially as relative movement occurs between glucose and the transmembrane helices. Movement of glucose in the cavity would presumably be accompanied by solvation and desolvation of the sugar and protein at specific sites as sugar−protein interactions form and break. Several amino acid residues in Glut1 whose possible interaction with glucose is consistent with experimental mutagenesis and SCAM results are shown in diagrammatic form in Figure 6. Note that not all potential substrate-binding residues in Glut1 have been analyzed, so that the residues shown represent an incomplete subset of candidates. The experimental constraints used to identify these residues were as follows. (1) The residue must be exposed on a helical face in contact with the external solvent as determined by pCMBS sensitivity. (2) Alteration of the side chain by mutagenesis must inhibit the rate of substrate influx. (3) The residue must possess a side chain that is capable of donating or accepting a hydrogen bond or possessing an aromatic side chain (in the case of interaction with the C-6 region of glucose). Most of the putative substrate-binding residues lie within the middle third of their respective helix. This is consistent with the cytoplasmic substrate-binding sites in the lac permease (*48*) and the glycerol-3-P antiporter (*49*) but was not used as an absolute constraint because of the uncertain location of the ends of the transmembrane segments. Additionally, as discussed above, the precise molecular interactions between the transporter and glucose may be altered with the commencement of the conformational change

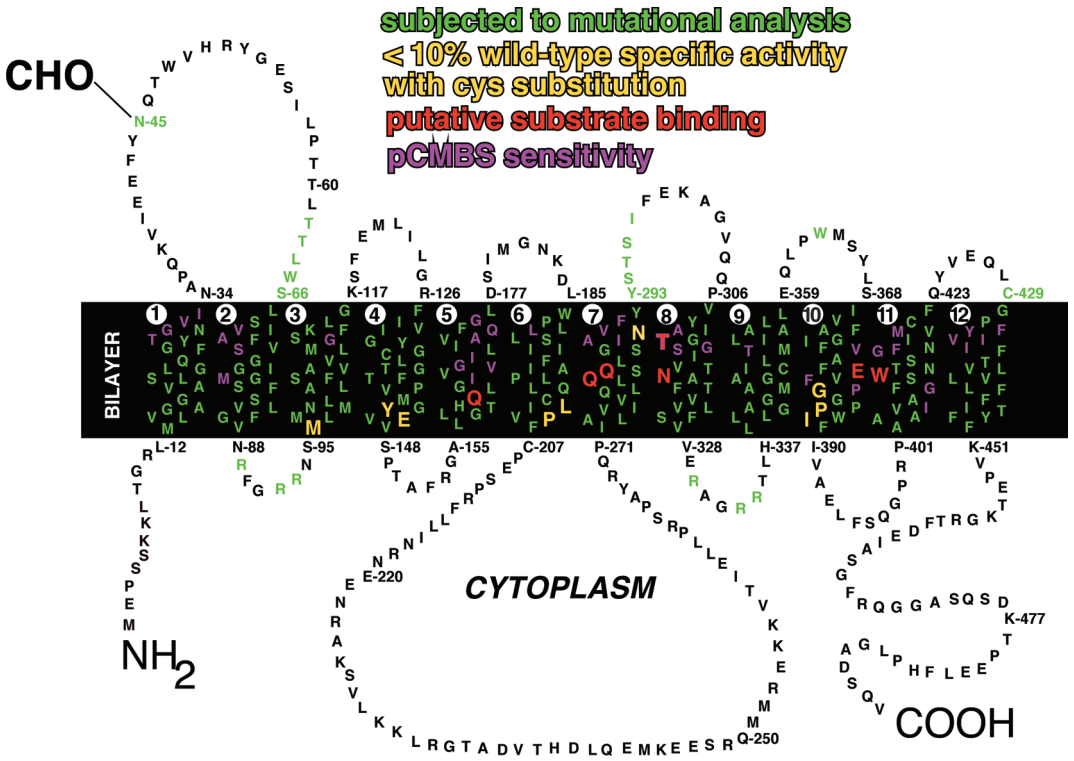

FIGURE 5: Summary of mutagenesis data and SCAM analysis of Glut1. The membrane is represented by a black rectangle, and the 12 transmembrane segments are numbered consecutively from the N-terminus to the C-terminus. The termini of the transmembrane segments are assigned as proposed in ref (*17*). Amino acid residues are identified by the single-letter code. Amino acid residues that have been subjected to mutagenesis are colored green. Residues that represent sites of pCMBS sensitivity are colored purple. Residues corresponding to mutations that inhibit transport activity by >90% are colored yellow. Putative substrate-binding residues are colored red. See the text for a detailed discussion.

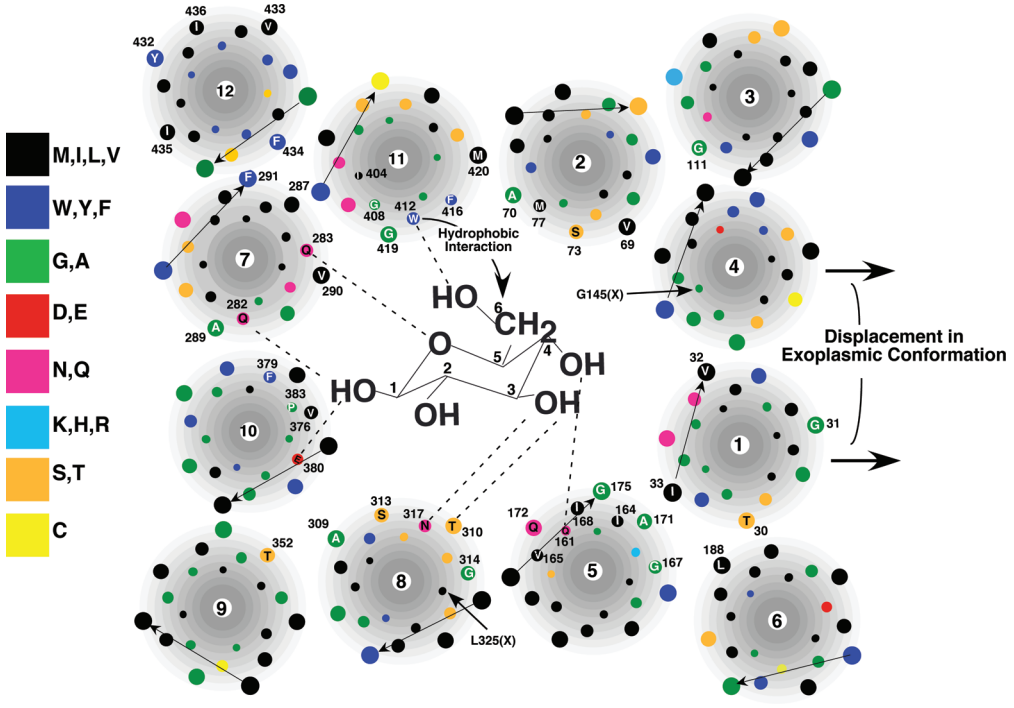

FIGURE 6: Low-resolution cartoon for the arrangement of the 12 transmembrane helices and of the exofacial binding site of Glut1. Proposed model of the exofacial glucose-binding site as viewed from the outside of the cell. For the sake of simplicity, all transmembrane segments are drawn as perfect helices perpendicular to the plane of the membrane. Glucose is not drawn to scale. The dotted lines represent possible hydrogen bonds formed between glucose hydroxyl groups and various side chains on Glut1. Numbered residues are accessible to pCMBS from the external solvent. The arrows on the right represent the probable displacement of helices 1 and 4 in the exofacial configuration of the transporter as compared to the cytoplasmic configuration. Residues in helices 4 (G145) and 8 (L325) that are within ~6 Å of each other as determined by chemical cross-linking experiments are indicated. Most helices are positioned such that their pCMBS-accessible residues face a proposed central cavity open to the extracellular fluid. Helices 1 and 12 exhibit no periodicity in their pCMBS reactivity. They are oriented such that only hydrophobic side chains face the lipid bilayer. The orientation of helices 4 and 8 is consistent with the results of chemical cross-linking experiments (*55*).

that ensues after initial substrate binding. This possibility is not addressed by the static crystal structures and represents a major challenge in deducing the mechanism of membrane transport. Because of the failure to meet the first constraint, no residues in helix 1 or 4 are predicted to be involved in exofacial substrate binding. As discussed above, each of the four contiguous outermost residues in helix 1 reacts with pCMBS, but this is likely because they actually reside in the exoplasmic fluid outside of the bilayer. Thus, the bulk of helices 1 and 4 may lie outside of the inner helical bundle in the exoplasmic configuration, as indicated by the rightward arrows in Figure 6, suggesting a difference between the cytoplasmic and exoplasmic folding patterns.

The biochemical data summarized here cannot unequivocally identify substrate-binding residues. However, the experimental evidence supporting a role for Q161, Q282, and W412 is reasonably compelling. Q161 is highly conserved among members of the Glut family, and substrate influx is dramatically inhibited by mutations at this site (*38*). Even the conservative substitution of an asparagine residue at this position reduces transport activity by 1 order of magnitude, indicating that the precise spatial positioning of the carbonyl and amide side chain groups is critical for function. Substitution of an asparagine at Q161 reduces the apparent affinity for the exofacial substrate-binding site of a nontransported glucose analogue by 18-fold. However, kinetic analysis is also consistent with Q161 residing at a critical spatial position such that mutations at this site inhibit the inward to outward conformational change of the unloaded transporter and thus tend to lock Glut1 into an inward-facing orientation (*38*). Similar kinetic and inhibitor analyses support a role for Q282 in exofacial substrate binding (*40*). However, the caveat concerning mutants at this site possibly being locked into the cytoplasmic configuration does not apply, because a leucine substitution at Q282 has no effect on transport activity, despite decreasing transporter affinity for exofacial ligands. This would not be the case if amino acid substitutions at this site inhibited the rate-limiting step involving the inward to outward conformational change. There is evidence that the QLS motif at positions 279−281 is involved in discriminating between glucose and fructose as substrates, perhaps by affecting hydrogen bond formation at the C-1 hydroxyl group (*64*). However, none of the QLS motif residues appears to be accessible to the external solvent, and thus, the motif may function to orient other residues in its vicinity that are directly involved in substrate binding. Because Q282 lies adjacent to the QLS motif in helix 7, it is possible that this residue forms a hydrogen bond with glucose at C-1 as indicated in Figure 6. Studies conducted more than 30 years ago with glucose analogues suggested that a Glut1 residue interacts with the C-6 position of the pyranose ring in a complex manner involving both polar and aromatic interactions (*62*), with a tyrosine or tryptophan residue being the most likely candidate. Of the tryptophan or tyrosine residues that are predicted to possess side chains that are facing the external aqueous cavity, W412 is the most likely to fulfill this function. Glycine, leucine, and cysteine substitutions at this site impair transport activity (*29*, *39*), whereas mutation of W412 to other aromatic residues (phenylalanine and tyrosine) has a minimal impact on transport activity (M. Mueckler, unpublished observations). W412 has been directly implicated in the photolabeling of Glut1 by the inhibitory ligand cytochalasin B (*41*). These observations suggest that an aromatic side chain is important at position 412 and are consistent with a role for W412 in substrate binding via interaction with the C-6 position. The seven putative substrate-binding residues are colored red in Figure 5. Interestingly, all of the side chains lie within the middle third of their respective transmembrane helices.

There is clearly a need to determine the structure of glucose transporters by X-ray diffraction analysis, a goal that has not yet been achieved for any eukaryotic MFS protein. Toward that end, we have developed a simple procedure that permits the purification of milligram quantities of monomeric recombinant mammalian glucose transporters expressed in *Pichia pasteuris*. Attempts at crystallization are ongoing.

ACKNOWLEDGMENT

We thank the members of the Mueckler laboratory for valuable discussions.

REFERENCES

(1) Joost, H.-G., Bell, G. I., Best, J. D., Birnbaum, M. J., Charron, M. J., Chen, Y. T., Doege, H., James, D. E., Lodish, H. F., Moley, K. H., Moley, J. F., Mueckler, M., Rogers, S., Schurmann, A., Seino, S., and Thorens, B. (2002) Nomenclature of the GLUT/SLC2A family of sugar/polyol transport facilitators. *Am. J. Physiol. 282*, E974–E976.

(2) Marger, M. D., and Saier, M. H. (1993) A major superfamily of transmembrane facilitators that catalyse uniport, symport and antiport. *Trends Biochem. Sci. 18*, 13–20.

(3) Pao, S. S., Paulsen, I. T., and Saier, M. H. (1998) Major facilitator superfamily. *Microbiol. Mol. Biol. Rev. 62*, 1–34.

(4) Saier, M. H. (2000) Families of transmembrane sugar transport proteins. *Mol. Microbiol. 35*, 699–710.

(5) Wood, I. S., and Trayhurn, P. (2003) Glucose transporters (GLUT and SGLT): Expanded families of sugar transport proteins. *Br. J. Nutr. 89*, 3–9.

(6) Scheepers, A., Joost, H. G., and Schurmann, A. (2004) The glucose transporter families SGLT and GLUT: Molecular basis of normal and aberrant function. *JPEN, J. Parenter. Enteral Nutr. 28*, 364–371.

(7) Kahn, B. B. (1996) Lilly lecture 1995. Glucose transport: Pivotal step in insulin action. *Diabetes 45*, 1644–1654.

(8) De Vivo, D. C., Wang, D., Pascual, J. M., and Ho, Y. Y. (2002) Glucose transporter protein syndromes. *Int. Rev. Neurobiol. 51*, 259–288.

(9) Santer, R., Schneppenheim, R., Dombrowski, A., Gotze, H., Steinmann, B., and Schaub, J. (1998) Fanconi-Bickel syndrome: A congenital defect of the liver-type facilitative glucose transporter. SSIEM Award. Society for the Study of Inborn Errors of Metabolism. *J. Inherited Metab. Dis. 21*, 191–194.

(10) Lowe, A. G., and Walmsley, A. R. (1989) The kinetics and thermodynamics of glucose transport in human erythrocytes. In Red Blood Cell Membranes (Agre, P., and Parker, J. C., Eds.) pp 597−634, Marcel Dekker, Inc., New York.

(11) Wheeler, T. J., and Hinkle, P. C. (1985) The glucose transporter of mammalian cells. *Annu. Rev. Physiol. 47*, 503–517.

(12) Cloherty, E. K., Heard, K. S., and Carruthers, A. (1996) Human erythrocyte sugar transport is incompatible with available carrier models. *Biochemistry 35*, 10411–10421.

(13) Cloherty, E. K., Hamill, S., Levine, K., and Carruthers, A. (2001) Sugar transporter regulation by ATP and quaternary structure. *Blood Cells, Mol., Dis. 27*, 102–107.

(14) Levine, K. B., Robichaud, T. K., Hamill, S., Sultzman, L. A., and Carruthers, A. (2005) Properties of the human erythrocyte glucose transport protein are determined by cellular context. *Biochemistry 44*, 5606–5616.

(15) Leitch, J. M., and Carruthers, A. (2007) ATP-dependent sugar transport complexity in human erythrocytes. *Am. J. Physiol. 292*, C974–C986.

(16) Kasahara, M., and Hinkle, P. C. (1977) Reconstitution and purification of the D-glucose transporter from human erythrocytes. *J. Biol. Chem. 252*, 7384–7390.

(17) Mueckler, M., Caruso, C., Baldwin, S. A., Panico, M., Blench, I., Morris, H. R., Allard, W. J., Lienhard, G. E., and Lodish, H. F. (1985) Sequence and structure of a human glucose transporter. *Science 229*, 941–945.

(18) Birnbaum, M. J., Haspel, H. C., and Rosen, O. M. (1986) Cloning and characterization of a cDNA encoding the rat brain glucose-transporter protein. *Proc. Natl. Acad. Sci. U.S.A. 83*, 5784–5788.
(19) Mueckler, M. (1994) Facilitative glucose transporters. *Eur. J. Biochem. 219*, 713–725.
(20) Carruthers, A. (1990) Facilitated diffusion of glucose. *Physiol. Rev. 70*, 1135–1176.
(21) Montel-Hagen, A., Kinet, S., Manel, N., Mongellaz, C., Prohaska, R., Battini, J. L., Delaunay, J., Sitbon, M., and Taylor, N. (2008) Erythrocyte Glut1 triggers dehydroascorbic acid uptake in mammals unable to synthesize vitamin C. *Cell 132*, 1039–1048.
(22) Hresko, R. C., Kruse, M., Strube, M., and Mueckler, M. (1994) Topology of the Glut 1 glucose transporter deduced from glycosylation scanning mutagenesis. *J. Biol. Chem. 269*, 20482–20488.
(23) Blodgett, D. M., Graybill, C., and Carruthers, A. (2008) Analysis of glucose transporter topology and structural dynamics. *J. Biol. Chem. 283*, 36416–36424.
(24) Pessino, A., Hebert, D. N., Woon, C. W., Harrison, S. A., Clancy, B. M., Buxton, J. M., Carruthers, A., and Czech, M. P. (1991) Evidence that functional erythrocyte-type glucose transporters are oligomers. *J. Biol. Chem. 266*, 20213–20217.
(25) Zottola, R. J., Cloherty, E. K., Coderre, P. E., Hansen, A., Hebert, D. N., and Carruthers, A. (1995) Glucose transporter function is controlled by transporter oligomeric structure. A single, intramolecular disulfide promotes GLUT1 tetramerization. *Biochemistry 34*, 9734–9747.
(26) Heinze, M., Monden, I., and Keller, K. (2004) Cysteine-Scanning Mutagenesis of Transmembrane Segment 1 of Glucose Transporter GLUT1: Extracellular Accessibility of Helix Positions. *Biochemistry 43*, 931–936.
(27) Olsowski, A., Monden, I., Krause, G., and Keller, K. (2000) Cysteine scanning mutagenesis of helices 2 and 7 in GLUT1 identifies an exofacial cleft in both transmembrane segments. *Biochemistry 39*, 2469–2474.
(28) Hruz, P. W., and Mueckler, M. M. (1999) Cysteine-scanning mutagenesis of transmembrane segment 7 of the GLUT1 glucose transporter. *J. Biol. Chem. 274*, 36176–36180.
(29) Hruz, P. W., and Mueckler, M. M. (2000) Cysteine-scanning mutagenesis of transmembrane segment 11 of the GLUT1 facilitative glucose transporter. *Biochemistry 39*, 9367–9372.
(30) Mueckler, M., and Makepeace, C. (1999) Transmembrane segment 5 of the Glut1 glucose transporter is an amphipathic helix that forms part of the sugar permeation pathway. *J. Biol. Chem. 274*, 10923–10926.
(31) Mueckler, M., and Makepeace, C. (2002) Analysis of transmembrane segment 10 of the Glut1 glucose transporter by cysteine-scanning mutagenesis and substituted cysteine accessibility. *J. Biol. Chem. 277*, 3498–3503.
(32) Mueckler, M., and Makepeace, C. (2004) Analysis of transmembrane segment 8 of the GLUT1 glucose transporter by cysteine-scanning mutagenesis and substituted cysteine accessibility. *J. Biol. Chem. 279*, 10494–10499.
(33) Mueckler, M., and Makepeace, C. (2005) Cysteine-scanning mutagenesis and substituted cysteine accessibility analysis of transmembrane segment 4 of the Glut1 glucose transporter. *J. Biol. Chem. 280*, 39562–39568.
(34) Mueckler, M., and Makepeace, C. (2006) Transmembrane segment 12 of the Glut1 glucose transporter is an outer helix and is not directly involved in the transport mechanism. *J. Biol. Chem. 281*, 36993–36998.
(35) Mueckler, M., and Makepeace, C. (2008) Transmembrane segment 6 of the Glut1 glucose transporter is an outer helix and contains amino acid side chains essential for transport activity. *J. Biol. Chem. 283*, 11550–11555.
(36) Mueckler, M., Roach, W., and Makepeace, C. (2004) Transmembrane segment 3 of the Glut1 glucose transporter is an outer helix. *J. Biol. Chem. 279*, 46876–46881.
(37) Mueckler, M., and Makepeace, C. (1997) Identification of an amino acid residue that lies between the exofacial vestibule and exofacial substrate-binding site of the Glut1 sugar permeation pathway. *J. Biol. Chem. 272*, 30141–30146.
(38) Mueckler, M., Weng, W., and Kruse, M. (1994) Glutamine 161 of Glut1 glucose transporter is critical for transport activity and exofacial ligand binding. *J. Biol. Chem. 269*, 20533–20538.
(39) Garcia, J. C., Strube, M., Leingang, K., Keller, K., and Mueckler, M. M. (1992) Amino acid substitutions at tryptophan 388 and tryptophan 412 of the HepG2 (GLUT1) glucose transporter inhibit transport activity and targeting to the plasma membrane in *Xenopus* oocytes. *J. Biol. Chem. 267*, 7770–7776.
(40) Hashiramoto, M., Kadowaki, T., Clark, A. E., Muraoka, A., Momomura, K., Sakura, H., Tobe, K., Akanuma, Y., Yazaki, Y., and Holman, G. D..; et al. (1992) Site-directed mutagenesis of GLUT1 in helix 7 residue 282 results in perturbation of exofacial ligand binding. *J. Biol. Chem. 267*, 17502–17507.
(41) Inukai, K., Asano, T., Katagiri, H., Anai, M., Funaki, M., Ishihara, H., Tsukuda, K., Kikuchi, M., Yazaki, Y., and Oka, Y. (1994) Replacement of both tryptophan residues at 388 and 412 completely abolished cytochalasin B photolabelling of the GLUT1 glucose transporter. *Biochem. J. 291*, 861–867.
(42) Liu, Q., Vera, J. C., Peng, H., and Golde, D. W. (2001) The predicted ATP-binding domains in the hexose transporter GLUT1 critically affect transporter activity. *Biochemistry 40*, 7874–7881.
(43) Olsowski, A., Monden, I., and Keller, K. (1998) Cysteine-scanning mutagenesis of flanking regions at the boundary between external loop I or IV and transmembrane segment II or VII in the GLUT1 glucose transporter. *Biochemistry 37*, 10738–10745.
(44) Schurmann, A., Doege, H., Ohnimus, H., Monser, V., Buchs, A., and Joost, H. G. (1997) Role of conserved arginine and glutamate residues on the cytosolic surface of glucose transporters for transporter function. *Biochemistry 36*, 12897–12902.
(45) Tamori, Y., Hashiramoto, M., Clark, A. E., Mori, H., Muraoka, A., Kadowaki, T., Holman, G. D., and Kasuga, M. (1994) Substitution at Pro385 of GLUT1 perturbs the glucose transport function by reducing conformational flexibility. *J. Biol. Chem. 269*, 2982–2986.
(46) Wellner, M., Monden, I., and Keller, K. (1994) The role of cysteine residues in glucose-transporter-GLUT1-mediated transport and transport inhibition. *Biochem. J. 299*, 813–817.
(47) Salas-Burgos, A., Iserovich, P., Zuniga, F., Vera, J. C., and Fischbarg, J. (2004) Predicting the three-dimensional structure of the human facilitative glucose transporter glut1 by a novel evolutionary homology strategy: Insights on the molecular mechanism of substrate migration, and binding sites for glucose and inhibitory molecules. *Biophys. J. 87*, 2990–2999.
(48) Abramson, J., Smirnova, I., Kasho, V., Verner, G., Kaback, H. R., and Iwata, S. (2003) Structure and mechanism of the lactose permease of *Escherichia coli*. *Science 301*, 610–615.
(49) Huang, Y., Lemieux, M. J., Song, J., Auer, M., and Wang, D. N. (2003) Structure and mechanism of the glycerol-3-phosphate transporter from *Escherichia coli*. *Science 301*, 616–620.
(50) Hresko, R. C., Murata, H., Marshall, B. A., and Mueckler, M. (1994) Discrete structural domains determine differential endoplasmic reticulum to Golgi transit times for glucose transporter isoforms. *J. Biol. Chem. 269*, 32110–32119.
(51) Marshall, B. A., Murata, H., Hresko, R. C., and Mueckler, M. (1993) Domains that confer intracellular sequestration of the Glut4 glucose transporter in *Xenopus* oocytes. *J. Biol. Chem. 268*, 26193–26199.
(52) Keller, K., Strube, M., and Mueckler, M. (1989) Functional expression of the human HepG2 and rat adipocyte glucose transporters in *Xenopus* oocytes. Comparison of kinetic parameters. *J. Biol. Chem. 264*, 18884–18889.
(53) Wellner, M., Monden, I., and Keller, K. (1995) From triple cysteine mutants to the cysteine-less glucose transporter GLUT1: A functional analysis. *FEBS Lett. 370*, 19–22.
(54) Yin, Y., He, X., Szewczyk, P., Nguyen, T., and Chang, G. (2006) Structure of the multidrug transporter EmrD from *Escherichia coli*. *Science 312*, 741–744.
(55) Alisio, A., and Mueckler, M. (2004) Relative proximity and orientation of helices 4 and 8 of the GLUT1 glucose transporter. *J. Biol. Chem. 279*, 26540–26545.
(56) van Iwaarden, P. R., Driessen, A. J., and Konings, W. N. (1992) What we can learn from the effects of thiol reagents on transport proteins. *Biochim. Biophys. Acta 1113*, 161–170.
(57) Abramson, J., Kaback, H. R., and Iwata, S. (2004) Structural comparison of lactose permease and the glycerol-3-phosphate antiporter: Members of the major facilitator superfamily. *Curr. Opin. Struct. Biol. 14*, 413–419.
(58) Wheeler, T. J., and Whelan, J. D. (1988) Infinite-cis kinetics support the carrier model for erythrocyte glucose transport. *Biochemistry 27*, 1441–1450.
(59) Brahm, J. (1983) Kinetics of glucose transport in human erythrocytes. *J. Physiol. 339*, 339–354.

(60) Taylor, L. P., and Holman, G. D. (1981) Symmetrical kinetic parameters for 3-O-methyl-D-glucose transport in adipocytes in the presence and in the absence of insulin. *Biochim. Biophys. Acta 642*, 325–335.
(61) Kaback, H. R., Dunten, R., Frillingos, S., Venkatesan, P., Kwaw, I., Zhang, W., and Ermolova, N. (2007) Site-directed alkylation and the alternating access model for LacY. *Proc. Natl. Acad. Sci. U.S.A. 104*, 491–494.
(62) Barnett, J. E. G., Holman, G. D., and Munday, K. A. (1973) Structural requirements for binding to the sugar-transport system of the human erythrocyte. *Biochem. J. 131*, 211–221.
(63) Kahlenberg, A., and Dolansky, D. (1972) Structural requirements of D-glucose for its binding to isolated human erythrocyte membranes. *Can. J. Biochem. 50*, 638–643.
(64) Seatter, M. J., De la Rue, S. A., Porter, L. M., and Gould, G. W. (1998) QLS motif in transmembrane helix VII of the glucose transporter family interacts with the C-1 position of D-glucose and is involved in substrate selection at the exofacial binding site. *Biochemistry 37*, 1322–1326.
(65) Lemieux, M. J. (2007) Eukaryotic major facilitator superfamily transporter modeling based on the prokaryotic GlpT crystal structure. *Mol. Membr. Biol. 24*, 333–341.